LOW ENERGY TRANSVERSE SAND BARS AT EL TRABUCADOR BEACH, EBRO DELTA. A PRELIMINARY STUDY.

Anna Mujal-Colilles[1], Manel Grifoll[2] and Albert Falqués[3]

Abstract

The complex rhythmic morphology of the inner side of the Trabucador barrier beach is investigated. This system features transverse bars along with shoreline undulations. From visual inspection, the typical spacing between bars is about 20 m and its length is similar. According to the literature they fall within the "Long transverse finger bars" type. However, this system is unique because there are many bars (~50 over 2 km of beach) and they are highly dynamic and persistent at the same time. A first characterization using orthophotos allows describing the existence of three main wavelength ranges: one at 15-25 m and one at 50-60 m, associated to the transverse bars, and another at 175-250 m, associated to the shoreline undulations. A preliminary discussion suggests that the dynamics of the bars and the shoreline undulations is probably dominated by feedbacks between morphology and both wave and wind driven currents.

Key words: Low energy beaches, alongshore rhythmic patterns, transverse bars, shoreline undulations, aerial orthophotos, morphodynamic self-organization.

1   Introduction

The morphology of sandy coasts, including the shoreline position and the bathymetry of the surf and shoaling zones, quite often displays complex and intriguing patterns. These patterns are sometimes nearly periodic alongshore or at least showing some sort of regularity with an alongshore recurrence length, *L*, and are then known as *rhythmic coastal morphologies*. Several types have been defined in the literature but the extreme complexity of beach dynamics and the increasing capacity and frequency of beach monitoring and field observations often challenge their traditional classification.

Sand bars extending perpendicularly to the coast or with an oblique orientation are known as *Transverse bars* . They usually occur in patches of a few of them up to tens, they are separated by troughs and they are typically attached to the shore. The alongshore spacing, *L*, is defined as the distance between successive bar crests. In the presence of an alongshore current, oblique bars may have its distal end shifted down-current or up-current with respect to the shore attachment and are then called down-current oriented or up-current oriented, respectively. With a dominant longshore current they tend to migrate downdrift with migration rates up to 40 m/d (Ribas and Kroon, 2007, Pellón et al., 2014). They sometimes show an asymmetry of their cross-section (the down-current flank being steeper than the up-current flank (Pellón et al., 2014). We can classify them in three types. The first one are *TBR bars*, which are associated to the Transverse Bar and Rip (TBR) state in the standard beach state classification (Wright and Short, 1984). They are typically wide and short-crested and their origin is the merging of the shallower sections of a crescentic bar into the beach. The second type are *medium energy finger bars*, which are sometimes observed in open microtidal beaches under medium-energy conditions (Konicki and Holman, 2000, Khabidov, 2001, Ribas and Kroon, 2007) and they always coexist with shore-parallel (or crescentic) bars. They are thin and elongated in contrast with the wider and shorter TBR bars. They are ephemeral (residence time from 1 day to 1 month), attached to the low-tide shoreline or, occasionally, to the shore-parallel bar. They are linked to the presence of alongshore wave driven current and they are up-current

---

[1] Civil and Environmental Department (UPC), Barcelona, Catalonia, Spain. anna.mujal@upc.edu
[2] Civil and Environmental Department (UPC), Barcelona, Catalonia, Spain. manel.grifoll@upc.edu
[3] Physics Department (UPC), Barcelona, Catalonia, Spain. albert.falques@upc.edu

oriented. Their spacing is in the range $L \approx$ 15 -200 m. Finally, the *Long Transverse Finger Bars* type (LTFB), which groups the 'large-scale finger bars' and the 'low-energy finger bars' of Pellón et al. (2014). They are characterized by long crests which are typically larger than the alongshore spacing which may vary in the range $L \approx$ 10 -500 m. They are generally observed to be persistent features in low to medium wave energy beaches, whose foreshore is a very flat terrace (Evans, 1938, Niedoroda and Tanner, 1970, Falqués, 1989, Bruner and Smosna, 1989, Gelfenbaum and Brooks, 2003). The wave focusing caused by refraction of shore-normal incident waves by the bars seems to be an essential process to them. Although they are most often observed on microtidal beaches, they can also exist on meso and macrotidal coasts (Levoy et al., 2013, Pellón et al., 2014).

In addition to surf/shoaling zone bathymetry, the shoreline itself can also display an alongshore rhythmicity in the form of undulations or cuspate shapes featuring apexes and embayments. Perhaps the most known are *beach cusps* that may develop at the swash zone with spacings $L \approx$ 1-50 m (Almar et al., 2008) but we are here interested in megacusps or even larger features. *Megacusps* are linked to crescentic or to transverse bars sharing the same alongshore spacing. In case of transverse bars, their apexes develop at the shore attachments of the bars and the embayments in between correspond to the troughs in between bars. But shorelines may also display undulations at a scale which is even larger than surf zone rhythmic bars, i.e., L >> X_b, where X_b is the width of the surf zone. They have been called *km-scale shoreline sand waves* (Idier and Falqués, 2014) because the typical wavelength in open ocean beaches is 1-10 km.

The origin and driving mechanisms of nearshore rhythmic patterns has been puzzling scientists for long. Their striking and relatively regular morphology along with its clear characteristic alongshore spacing in spite of the multi-scale high complexity of coastal dynamics suggests that something important occurs in the physics at that particular length scale. The most common assumption in the past was that a pre-existing template in the hydrodynamics (currents and/or waves) imprints its particular pattern on the morphology (Holman and Bowen, 1982). However, it has been shown that rhythmic morphologies can emerge from internal instabilities of the coupling between morphology and hydrodynamics through the sediment transport (Coco and Murray, 2007, Ribas et al., 2015). This has been shown for crescentic bars (Falqués et al., 2000, Deigaard et al., 1999, Calvete et al., 2005, Garnier et al., 2008), transverse bars (Garnier et al., 2006, Ribas et al., 2012), beach cusps (Coco et al., 2000, Dodd et al., 2008) and km-scale shoreline undulations (Ashton et al., 2001, Falqués and Calvete, 2005, van den Berg et al., 2012, Kaergaard and Fredsoe, 2013), and is known as the *self-organization theory*.

Checking the self-organization explanation for alongshore rhythmic features is in general not easy, since it needs frequent and detailed bathymetric surveys along with measurements of currents and waves during the time where the features are incipient. Thus, providing detailed and high quality data on rhythmic morphology development and dynamics is strongly valuable. The southwestern flank of the Ebro delta (Catalonia, Spain) features a long spit or barrier beach called Trabucador beach, which separates the Alfacs basin from the open Mediterranean sea. At its inner shore facing the Alfacs basin the Trabucador barrier beach commonly displays transverse bars with a typical alongshore spacing of tens of meters and a similar cross-shore length. At the same time, aerial photos also show the presence of larger scale shoreline undulations, up to ~ 250 m. This beach can be considered as "low-energy" since it is sheltered from the Mediterranean waves. A preliminary description of this morphological system was done by Falqués (1989) and aerial orthophotos are available since 1946. The aim of the present paper is a description of the characteristics of this system. We suspect that the morphology and the length scales of this system are largely self-organized and this contribution is a preliminary step towards determining which are the physical mechanisms driving its formation and dynamics. We analyze the shorelines from aerial orthophotos during the period 1946-2016 (source *Institut Cartogràfic i Geològic de Catalunya,* ICGC) along with occasional field observations by one of the authors during the period 1986-2016, (Falqués, 1989).

2   Study area

The Ebro delta is located in the western Mediterranean sea, NE of the Iberian peninsula, in Catalonia (Spain) (see Figure 1). The present day delta is relatively recent (about 600 yr), extends around 25 km offshore and has an area of about 325 km^2. On the lateral margins it features two spits, one trending to the NE, El Fangar, another trending to the SW and consisting of the Trabucador barrier beach and La Banya peninsula. Between the southwestern spit (Trabucador and La Banya) and the mainland, there is a semi-enclosed bay called Alfacs bay. It is nearly rectangular about 16 km long and 4 km wide, with an average depth of about 4 m (6.5 m in the center of the bay). The Alfacs Bay can be geomorphologically classified as a bar-built estuary formed by the sediment discharge from the Ebro River in combination with wave action (Pritchard, 1952). The bed is made of silt and clay (Palacin et al., 1991). However, next to the inner side of the Trabucador barrier beach there is a sandy and shallow shelf that is composed of fine sand with $D_{50} \approx 0.15\text{-}0.3$ mm (Falqués, 1989). This shelf deepens from 0 to roughly 1 m within about 125 m width and it has been built out of sediments from the outer side of the beach during overwash events (see Figure 1). The mean bed slope near the shoreline is about $\beta = 0.01$.
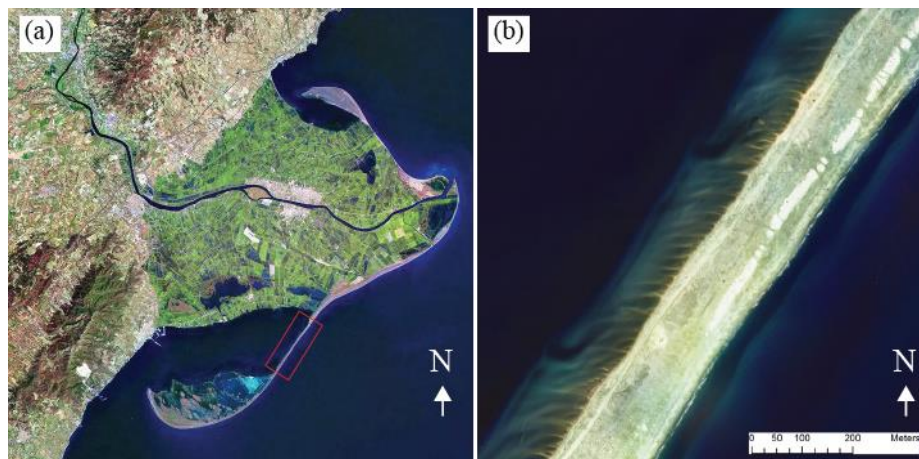

Figure 1. a) Ebro Delta; b) Zoom view of the Trabucador barrier beach in 2012. The shallow shelf with the trans-verse bars can be seen at the inner side (to the left). Image from ICGC.

3   Methodology

3.1   *Field observations*

Shoals and sand bars are usually present in the shallow shelf at the inner side of the Trabucador barrier beach, where water depths are less than roughly 1 m. Bars are typically elongated and with different orientations, most of them trend however to the west, nearly perpendicular to the coastline. At the same time, the shoreline is sinuous featuring many undulations with alongshore wavelengths ranging from about 20 m to 250 m. Many of these undulations are linked to the shore attachments of the bars. Falqués (1989) reported a first description of this morphology, based on maps, aerial photos and direct field observations in August 1986 and September 1988. More detailed characteristics of the system are:

    a)   Bars: There are many bars, about ~ 50 over 2 km beach. They are mainly rotated to the left with respect to shore normal viewing from the beach (an angle $\sim 10\text{-}40°$), i.e., they trend approximately to the W. Many of them reach the coastline and a megacusp develops at the attachment point (see Figure 2). Both their length and alongshore spacing ranges roughly between 5 m and 100 m but are typically of 15-30 m. Their vertical relief can reach about 0.4 m. They are inter-tidal, becoming mostly emerged at low tide. As can be seen in the aerial photos, the whole bar system usually extends offshore into the Alfacs basin all across the shallow shelf, i.e., about 125 m. According to

the aerial pictures and to direct inspection they are quite persistent, sometimes they are very visible, sometimes they are less, sometimes it seems that they are not present. According to local fishermen, they have been there for at least 50 or 60 years. Indeed, they are already visible in an aerial photo of 1946. According to the existing literature on bars observed at other sites, these bars fit into the LTFB type.

b) Large scale shoreline undulations: Small megacusps develop at the bar attachments to the shoreline. These megacusps can be quite big in case of the largest bars and correspond to the capes of relative-ly large undulations that are visible in the aerial photos. The wavelengths of these undulations are somewhat larger than the typical alongshore spacing of the bars, in the range 60-250 m, so that there are also smaller bars in the embayments between the capes.

A. Falqués and colleagues made a bathymetric map of a beach section with 4 bars in August 1986 (see Figure 3). The angle of the bars with the shore normal was 14°, 24°, 19° to the left viewing from the beach. The bars had an asymmetric cross-bar profile steeper at the NE side and milder at the SW side. The alongshore spacing was about 60-70 m. At the trough between two main bars there was a secondary minor bar not connected to the shoreline. Shoreline undulations or megacusps were associated to the bar attachment to the shoreline.

Figure 2. Pictures of some bars at low tide during 1986-1988. a) a series of 5 bars and b) view of one bar from the shoreline, clearly showing the wave focusing phenomenon.
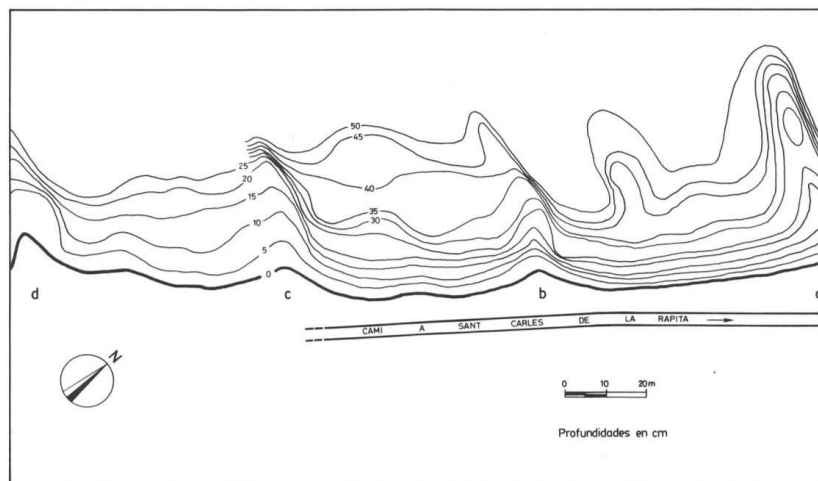

Figure 3. Bathymetry of a series of bars surveyed in August 1986. Depth contours in cm.

3.2   *Aerial orthophotos and image processing*

The identification of the mean distance between bars is obtained with an accurate analysis of 16 geo-referenced orthophotos from the *Institut Cartogràfic i Geològic de Catalunya* (ICGC). Images are available from 1946 to 2015 without a regular flight frequency over the Ebro Delta until 2007. Figure 4 illustrates the quality of the images along the period of the research, where the bars are clearly present. However, some other images did not have quality enough to obtain the wavelength of the LTFB bars (see Figure 5) but will be used to describe large scale shoreline undulations
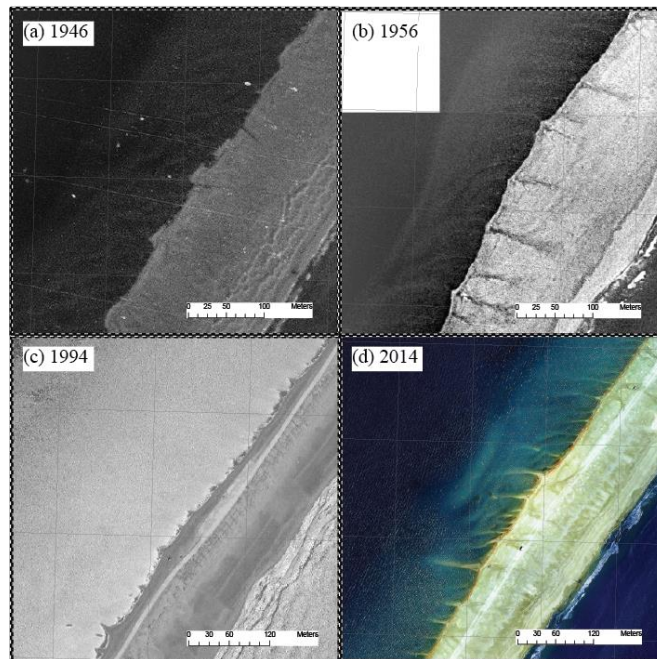

Figure 4. Evolution of the bars from photos taken in a)1946, b)1956, c)1994 and d)2014. Orthophotos from ICGC.
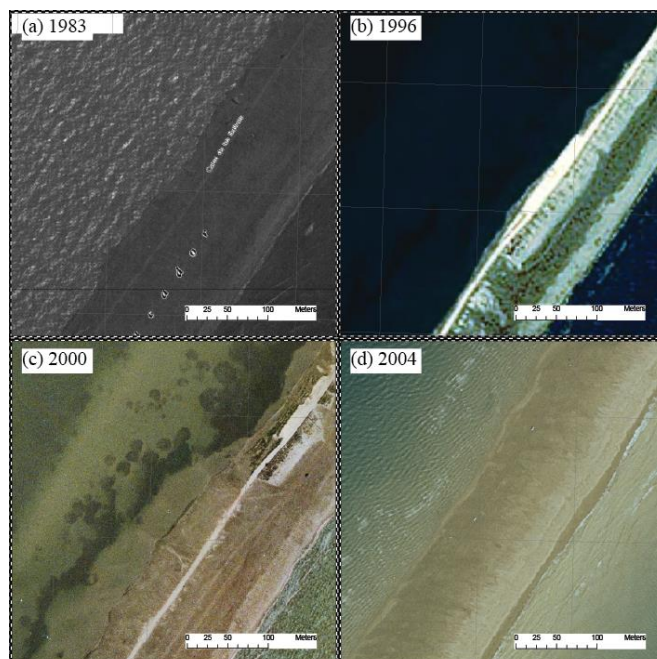

Figure 5. Selection of low quality images. a)1983, b)1996, c)2000 and d)2004. Orthophotos from ICGC.

After shoreline profiling using GIS software, data-points are rotated using a permanent road in the Trabucador barrier beach as reference axis. Raw data-points are then interpolated in an equally-spaced shoreline evolution vector. The energy spectra of the interpolated shoreline is computed in order to obtain the dominant wavelengths. The interpolated shoreline data are also filtered (low-pass and high-pass) to identify visually the temporal evolution of these undulations and to corroborate the wave-lengths that are provided by the spectral analysis. The Fourier analysis of the inner side of the Trabucador beach is performed in a 2 km segment length.

Preliminary results using the described methodology indicate the permanent existence of three peaks in the energy spectra around 20 meters wavelength, 50 meters and 200 meters in most of the orthophotos, with sporadic peaks in individual images.

3.3 Hydrodynamics and sediment transport characterization

3.3.1 Meteorology

The wind regime in the Ebro Delta is characterized by the prevalence of North-westerly winds during autumn and winter and onshore winds (sea-breeze) during summer (Grifoll et al., 2016, Cerralbo et al., 2015a). Using one-year observed wind data, Grifoll et al. (2015) estimate the monthly percentage of time of North-westerly winds: during winter this percentage was about the 80% decreasing during summer until 20%. However, in the southern margin of the Ebro delta (where Trabucador beach is located), NW winds may be altered due to the presence of the local topography (Cerralbo et al., 2015a).

3.3.2 Waves

Because this beach is sheltered waves are usually very small. Figure 6 and Figure 7 show preliminary numerical results obtained from the implementation of SWAN model in the stationary mode (Booij et al., 1996). Maximum wave heights of $H_s \sim 0.35$ m can be reached during the strong NW wind events or intense SW breezes. Nevertheless, a striking and very persistent process is wave focusing by the bars due to topographic refraction. As shown in Figure 2b, the small waves approaching the bars strongly refract, the wave crests turn towards the bar crest and cross the wave crests coming from the other bar flank. This creates a zone with small breakers over the bar crest and a quite strong onshore current over the bar. In calm conditions, when the waves are exceedingly small and imperceptible far from the bars, they seem to be generated near the bars where their energy focuses by refraction. This process was clearly described by Niedoroda and Tanner (1970) and was suggested to be one of the driving mechanisms of the bars. Quantitative analysis of this hypothesis has been subsequently done by Garnier et al. (2006) (see also Ribas et al., (2015)).
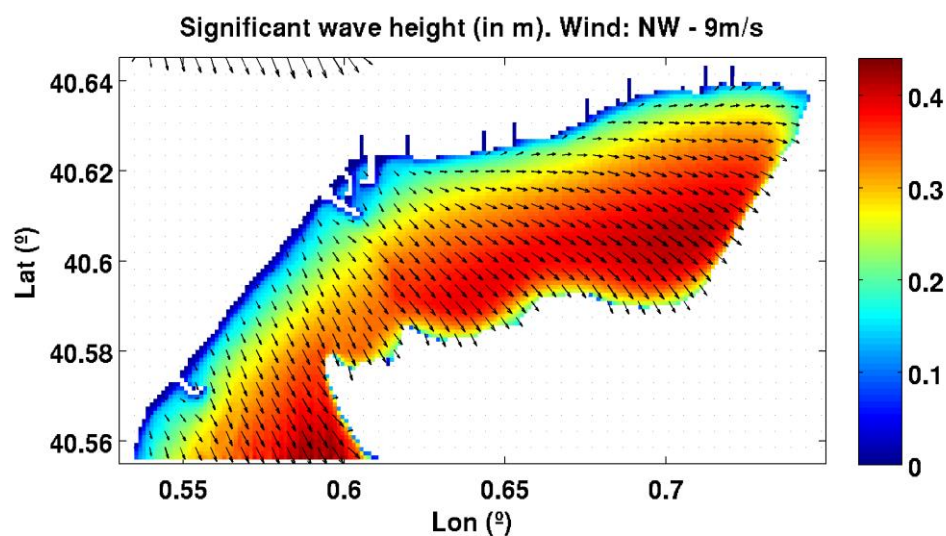

Figure 6. Significant wave height and wave propagation direction (black arrows) for NW wind direction.
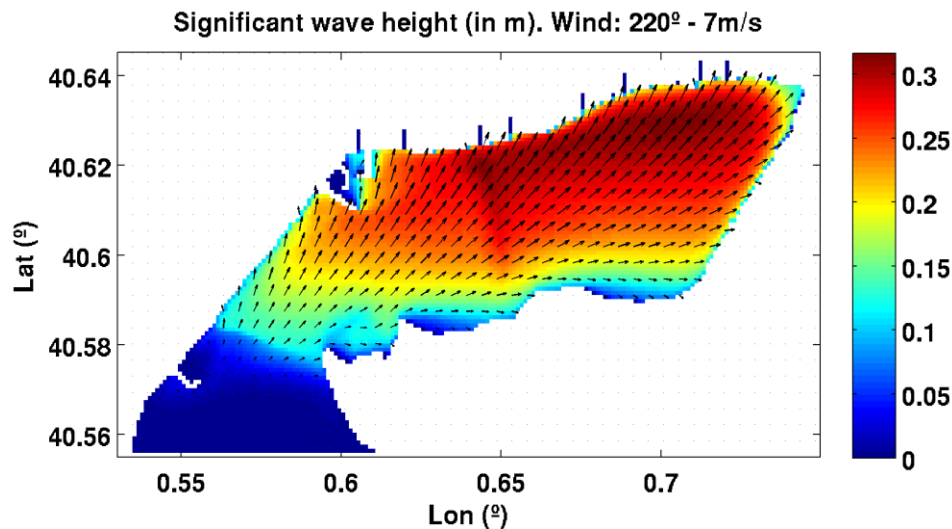
Figure 7. Significant wave height and wave propagation direction (black arrows) for SW sea-breeze wind.

3.3.3   Tides

The observed tidal range during 21st, 22nd and 23rd September, 1988, was about 0.28 m. The tide was mainly diurnal with T=24.8 h and with a harmonic of T=12.4 h. A secondary sea level variability of 0.08 m was also observed with T=3.8 h. Approximate computations show that this is roughly the period of the lowest resonance mode of the Alfacs bay. A similar period, but somewhat smaller (3.2-3.5 h), has been confirmed by other studies, see, e.g., Cerralbo et al. (2014) and Cerralbo et al. (2015). The first seiching mode, with a period of about 1 h has been also been reported by these two papers.

3.3.4   Currents

The water circulation in Alfacs at short temporal scales (orders of hours) is dominated by the local wind and the seiche activity (Cerralbo, 2015). For large temporal scales the water response is originated by a combined effect of a gravitational circulation due to freshwater inputs and the residual effect of winds. No measurements of currents are available at the shelf where bars are located but the currents were estimated with passive tracers during the field campaign of September 1988. With North wind of 7.3 m/s a maximum current of 0.30-0.35 m/s to the SW was observed over the crest of a bar with water depth of 0.05-0.1 m. The current was clearly favored by the breaking of the small waves over the bar. At the same time, at the deeps between the bars with 0.3-0.5 m depth currents of 0.15-0.20 m/s were observed. The maximum current in the opposite direction was about 0.2 m/s with 6.1 m/s wind from the S-SE. This beach is microtidal, with tidal range ~ 0.25 m, but seiches are important. Cerralbo (2015) measured currents up to more than 0.5 m/s close to the mainland shore in front of the Trabucador beach, which were associated to the 0th or 1st seiche modes of the Alfacs bay. However, the Trabucador beach is nearly an antinode for these modes so that the seiching currents should be very small.

3.3.5   Sediment and bar mobility

An indirect proof of the water flow and associated sediment transport is the presence of many ripples. In September 1988 it was observed how the shape of a bar changed and how it migrated about 0.4 m within less than 20 hours. The migration was consistent with the asymmetry in cross-bar shape, towards the steepest side. We also observed how the ripples at the bar crest formed, changed the shape and size and disappeared.

4   Discussion

We here discuss some physical mechanisms that could have originated the rhythmic morphological system and/or could be driving its dynamics at present.

4.1   Bed-surf instability mechanism

In case of normal or nearly normal wave incidence, alongshore bathymetric gradients cause differential breaking along the shore creating rip currents. If the corresponding sediment transport is such that a positive feedback occurs between the circulation and the bathymetric features, rhythmic bars can emerge from it. This was called bed-surf instability mechanism (Falqués et al., 2000) and has been recognized as the origin of crescentic bars although it can also give rise to transverse bars (Garnier et al., 2006). A clear example of the hydrodynamic counterpart of this mechanism is the wave focusing over the bars by bathymetric wave refraction observed at the Trabucador beach, which is a very striking and persistent process (see Section 3.3.2). This is an indication that bed-surf instability mechanism should be active. Currents of about 0.35 m/s and sediment mobility (mainly bed-load) associated to it have been observed (Falqués, 1989). Thus, this instability could be the origin of such bars and, at least, it seems that the related processes affect them.

During strong NW events, where wave incidence is normal or nearly normal, see Figure 6, this mechanism should be quite strong too. According to instability models, the wavelength of the emerging rhythmic bars scale with the width of the surf zone, $L \sim X_b$ (Garnier et al., 2006, Ribas et al., 2012). This scaling is consistent with the wavelengths observed at El Trabucador beach, $L \sim 20$ m, if we assume $H_{rms} \approx$ 0.1 m. Indeed, assuming a common value for the breaking index, $\gamma_b = 0.5$, the surf zone width would be of $X_b \approx H_{rms} / \beta \gamma_b \approx 20$ m.

4.2   Bed-flow instability mechanism

For oblique wave incidence, such as the results shown in Figure 7, alongshore bathymetric gradients cause acceleration/decceleration and deflection of the longshore current as it would happen with dunes or by alternate bars in an alluvial channel. This current can be driven by the obliquely incident breaking waves but also by the wind or other causes. Again, if the corresponding sediment transport induces a positive feedback, rhythmic bars can emerge from it. In case of normal wave incidence, only the bed-surf mechanism can act, the bed-flow mechanism cannot occur. However, for oblique wave incidence both mechanisms may coexist and the distinction between both is just conceptual. Garnier et al. (2006) (see also references therein and the review in Ribas et al. (2015)) have shown that bed-flow and bed-surf mechanisms can generically originate transverse bars. More specifically, Ribas (2012) found that the medium energy finger bars could be explained following this hypothesis. The asymmetric cross-bar shape of the bars (Falqués, 1989) clearly suggests the action of a current as main driving mechanism or at least in shaping them once initiated. Indeed, in the bathymetry of August 1986 (Figure 3) the steepest flank was the NE one, suggesting a current directed to the NE (as can be inferred from Figure 7). Also, the observed migration of the bars (Falqués, 1989) suggests that currents shape them. However, the origin of the currents seems unclear. Tidal currents are negligible and the currents due to the seiches should also be very small since the inner Trabucador beach is nearly an antinode (Cerralbo et al., 2014). Another possible forcing of appreciable alongshore currents at the Trabucador beach would be the wind, mainly from the SW (e.g., strong sea breeze during summer days) or perhaps NE winds, which are strong and relatively common in winter. The currents forced by these winds would be reinforced by the breaking of the obliquely incident small wind waves.

4.3   High-angle wave shoreline instability mechanism

For oblique wave incidence, bathymetric perturbations of the shoaling zone cause alongshore gradients in refraction and shoaling. This induces alongshore gradients on the breaking waves. Thereby gradients in littoral drift cause erosion/accretion patterns in the surf zone. When a large scale shoal (size $\gg X_b$) develops at the surf zone the cross-shore beach profile becomes out of equilibrium and the sand tends to

diffuse offshore to recover a new equilibrium profile. On the contrary, if a deficit of sand occurs, sand from the shoreface tends to move onshore for the same reason. Thus, the bathymetric perturbations in the surf zone tend to induce perturbations in the shoaling zone so that a positive feedback can occur. Thus, a coupled pattern in the morphology (surf-shoaling zones) and in the wave field grows. This can cause alongshore sand waves with shoreline undulations with a wavelength $L >> X_b$, which on open ocean beaches is in the order $L \sim 1\text{-}10$ km. This mechanism has been extensively studied (see, e.g., Ashton et al. (2001), Falqués and Calvete (2005), Idier et al. (2011)) and the instability typically develops for high-angle waves, i.e., angles between the propagation direction and the shore normal $> \approx 42^o$ at the depth of closure. For the small waves reaching the Trabucador beach the possible length scales would be significantly reduced. First, the break of the shelf would be of about 1 m, so that it would be the wave base for waves of $\lambda \approx 2$ m. This shallow shelf would be the shoaling zone for such small waves. Computations with the 1D-morfo model (Falqués and Calvete, 2005) were done by assuming H_s=0.07 m, T_p=0.8 s and an angle between wave fronts and shoreline θ=70°. The depth of closure was assumed to be D_c=0.3 m. Then, a dominant wavelength $L \approx 157$ m, a characteristic growth time of 180 d and a migration celerity 0.35 m/d were obtained. Thus, this mechanism could not be the driver of transverse bars because of the mismatch in alongshore lengthscales but it could affect the larger scale shoreline undulations in case of SW winds.

4.4   *Infragravity edge waves*

Holman and Bowen (1982) proposed that combinations of infragravity edge waves could imprint rhythmic patterns in the surf zone bathymetry that were similar to crescentic bars or transverse bars. This hypothesis for the formation of these patterns has, however, some shortcomings (Coco and Murray, 2007). In particular it disregards the feedback of the incipient morphologic patterns into the hydrodynamics and has therefore been generally abandoned. Nevertheless, Falqués (1989) examined the possibility that a 0-mode edge wave could have originated the alongshore rhythmicity of the transverse bar system at El Trabucador. The conclusion was that the generating edge waves should have periods in the range T $\sim$ 25-115 s, which is much longer than the small wind waves reaching the beach and it is therefore not clear which could be the mechanism to generate and to maintain such long waves. One might think of the seiches, e.g., the first mode with T$\approx$ 1 h, which is very energetic (Cerralbo et al., 2015). But the wavelength would then be about 100 km (Falqués, 1989), which is totally out of order. In any case, it would be interesting to measure possible infragravity sea level oscillations at the band 20-120 s at this beach.

4.5   *Forcing by ocean rhythmic bars during overwash/breaching*

During severe storms from the E or NE the Trabucador barrier beach is sometimes flooded and breached. Overwash fans can then occur and these sand bodies can become the observed bars or at least some of the largest ones. Perhaps this might act as an initial perturbation and initiate the feedback mechanisms between morphology and hydrodynamics that later on could create more bars and induce the alongshore periodicity. The orientation of the bars, roughly from E to W, would support this hypothesis. Even the over-wash/breaching process itself could be modulated by rhythmic patterns in the surf zone of the open sea side and the corresponding alongshore rhythmicity could be imprinted in the inner morphology.

5   Conclusions

Field observations at the inner side of the Trabucador barrier beach show the existence of a complex rhythmic morphological pattern featuring LTFB bars and shoreline undulations with alongshore wavelengths in the range $\sim$ 10-250 m. The most frequent wavelength in the bar system is about 20 m while the wavelength of the undulations tends to be larger, up to 250 m. Aerial orthophotos show that this system exists at least since 1946. Preliminary results of the Fourier analysis confirm the predominance of two main energetic peaks along the 16 analyzed images. The first peak is around 20 meters wavelength but can vary from 15 to 25 meters depending on the year. This peak is associated to the LTFB bars and it is confirmed by the visual inspection of Falqués (1989). The second peak, is of the order of 50 meters being computed in all the orthophotos within a range of 50-60 meters. The third peak is located around 200

meters in the range from 175 to 250 meters, and is present in 12 of the 16 orthophotos

The wave focusing by the bars due to topographic refraction seems to be a key process for bar formation and maintenance as suggested by Niedoroda and Tanner (1970). This indicates that the bed-surf instability mechanism (Falqués et al., 2000) could be the main driver of the LTFB bars. This is especially so during the strong NW events, when wave incidence is normal or nearly normal. Furthermore, the 20 meters observed dominant wavelength is roughly consistent with modelling by Garnier et al. (2006). Observations also suggest that alongshore currents, especially during SW wind events, could be important. The larger scale shoreline undulations are intriguing; some of them are linked to the largest LTFB bars and could therefore obey to a lengthscale coarsening process associated to the bars. However, since the SW waves have a large incidence angle they could trigger the high-angle wave instability (Ashton et al., 2001) in which case wavelengths in the order of 200 m could emerge (Falqués and Calvete, 2005). It is also possible that breaching or/and overwash of the barrier beach during severe storms play a role on the inner rhythmic system.

Acknowledgements

References

Almar, R., Coco, G., Bryan, K.R., Huntley, D.A., Short, A.D. and Senechal, N., 2008. Video observations of beach cusp morphodynamics, *Mar. Geology,* 254: 216-223.

Ashton, A., Murray, A. B. and Arnault, O., 2001. Formation of coastline features by large-scale instabilities induced by high-angle waves, *Nature*, 414: 296-300.

Booij, N., Holthuijsen, L.H. and R.C. Ris, 1996. The SWAN wave model for shallow water, *Proc. 25th Int. Conf. Coastal Engng.*, Orlando, USA, vol. 1, 668-676.

Bruner, K.R. and Smosna, R.A., 1989. The movement and stabilization of beach sand on transverse bars, Assateague Island, Virginia. *J. Coastal Res.,* 5(3):593-601.

Calvete, D., Dodd, N., Falqués, A. and van Leewen, S.M., 2005. Morphological Development of Rip Channel Systems: Normal and Near Normal Wave Incidence. *J. Geophys. Res.,* 110(C10006), doi:10.1029/2004JC002803.

Cerralbo, P., Grifoll, M., Valle-Levinson, A. and Espino, M., 2014. Tidal transformation and resonance in a short, microtidal Mediterranean estuary (Alfacs Bay in Ebre delta). *Estuarine, Coastal and Shelf Science*, 145: 57-68.

Cerralbo, P., Grifoll, M. and Espino, M., 2015. Hydrodynamic response in a microtidal and shallow bay under energetic wind and seiche episodes. *J. Marine System*, 149:1-13.

Cerralbo, P., Grifoll, M., Moré, J., Bravo, M., Sairouní Afif, A. and Espino, M., 2015a. Wind variability in a coastal area (Alfacs Bay, Ebro River delta). *Adv. Sci. Res.*, 12:11-21.

Coco, G., Huntley, D.A. and O'Hare, T.J., 2000. Investigation of a self-organization model for beach cusp formation and development. *J. Geophys. Res.*, 105(C9): 21991-22002.

Coco, G. and Murray, A.B., 2007. Patterns in the sand: From forcing templates to self-organization. *Geomorphology*, 91:271-290.

Deigaard, R., Dronen, N., Fredsoe, J., Jensen, J.H. and Jorgensen, M.P., 1999. A morphological stability analysis for a long straight barred coast. *Coastal Eng.*, 36(3):171-195.

Dodd, N., Stoker, A., Calvete, D. and Sriariyawat, A., 2008. On Beach Cusp Formation. *J. Fluid Mech.*, 597:145-169.

Evans, O.F., 1938. The classification and origin of beach cusps. *J. Geology*, 46:615-627.

Falqués A., 1989. Formación de Topografía rítmica en el Delta del Ebro. *Rev. Geofísica*, 45 (2): 143-156.

Falqués, A., Coco, G. and Huntley, D.A., 2000. A mechanism for the generation of wave-driven rhythmic patterns in the surf zone. *J. Geophys. Res.*. 105(C10):24071-24088.

Falqués, A. and Calvete, D., 2005. Large scale dynamics of sandy coastlines. Diffusivity and instability. *J. Geophys. Res.*, 110(C03007), doi:10.1029/2004JC002587.

Garnier, R., Calvete, D., Falqués, A. and Caballeria, M., 2006. Generation and nonlinear evolution of shore-oblique/transverse sand bars. *J. Fluid Mech.*, 567:327-360.

Garnier, R., Calvete, D., Falqués, A. and Dodd, N., 2008. Modelling the formation and the long-term behavior of rip channel systems from the deformation of a longshore bar. *J. Geophys. Res.*, 113(C07053), doi:10.1029/2007JC004632.

Gelfenbaum, G. and Brooks, G.R., 2003. The morphology and migration of transverse bars off the west-central Florida

coast. *Mar. Geology,* 200:273-289.

Grifoll, M., Navarro, J., Pallares, E., Ràfols, R., Espino, M. and Palomares, A., 2016. Ocean–atmosphere–wave characterisation of a wind jet (Ebro shelf, NW Mediterranean Sea). *Nonlin. Processes Geophys.*, 23:143-158.

Holman, R.A. and Bowen, A.J., 1982. Bars, bumps, and holes: models for the generation of complex beach topography. *J. Geophys. Res.* 87(C1):457-468.

Idier, D., Falqués, A., Ruessink, B.G. and Garnier, R., 2011. Shoreline instability under low-angle wave incidence. *J. Geophys. Res.*, 116(F04031), doi:10.1029/2010JF001894.

Idier, D. and Falqués, A., 2014. How kilometric sandy shoreline undulations correlate with wave and morphology characteristics: preliminary analysis on the Atlantic coast of Africa. *Adv. Geosciences*, 39:55-60.

Kaergaard, K. and Fredsoe, J., 2013. Numerical modeling of shoreline undulations part 1: Constant wave climate. *Coastal Eng.*, 75:64-76.

Khabidov, A., 2001. Transverse bars formation on a tideless beach. *Proceedings Coastal Dynamics 2001*, American Society of Civil Engineers. Lund, Sweden, 666–672.

Konicki, K.M. and Holman, R. A., 2000. The statistics and kinematics of transverse bars on an open coast. *Mar. Geology*, 169:69-101.

Levoy, F., Anthony, E.J., Monfort, O. Robin, N. and Bretel, P., 2013. Formation and migration of transverse bars along a tidal sandy coast deduced from multi-temporal Lidar datasets. *Mar. Geology,* 342:39-52.

Niederoda A.W. and. Tanner W. F, 1970. Preliminary study on transverse bars. *Mar. Geology*, 9: 41-62.

Palacin, C., Martin, D. and Gili, J. M., 1991. *Marine Biol.*, 110(2): 315-321.

Pellón, E., Garnier, R. and Medina, R., 2014. Intertidal finger bars at El Puntal, Bay of Santander, Spain: observation and forcing analysis. *Earth Surf. Dynamics*, 2: 349-361.

Pritchard, A., 1952. *Estuarine Hydrography. Advances in Geophysics, vol. 1*. Academic Press, Inc., New York.

Ribas, F. and Kroon, A., 2007. Characteristics and dynamics of surfzone transverse finger bars. *J. Geophys. Res.*, 112(F03028), doi:10.1029/2006JF000685.

Ribas, F., de Swart, H.E., Calvete, D. and Falqués, A., 2012. Modeling and analyzing observed transverse sand bars in the surf zone. *J. Geophys. Res.*, 117 (F02013), doi:10.1029/2011JF002158.

Ribas, F., Falqués, A., de Swart, H.E., Dodd, N., Garnier, R. and Calvete, D., 2015. Understanding coastal morphodynamic patterns from depth-averaged sediment concentration. *Rev. Geophys.*, 53, doi:10.1002/2014RG000457.

Van den Berg., N., Falqués, A. and Ribas, F., 2012. Modelling large scale shoreline sand waves under oblique wave incidence. *J. Geophys. Res.*, 117(F03019), doi:10.1029/2011JF002177.

Van Enckevort, I.M.J., Ruessink, B.G., Coco, G., Suzuki, K., Turner, I.L., Plant, N.G. and Holman, R.A., 2004. *J. Geophys. Res.*, 109(C06028), doi:10.1029/2003JC002214.

Wright, L.D. and Short, A.D., 1984. Morphodynamic variability of surf zones and beaches: A synthesis. *Mar. Geology,* 56:93-118.